Asociación Argentina
de Mecánica Computacional

Mecánica Computacional Vol XXVII, págs. 33-48 (artículo completo)
Alberto Cardona, Mario Storti, Carlos Zuppa. (Eds.)
San Luis, Argentina, 10-13 Noviembre 2008

AN INTERFACE CAPTURING FINITE ELEMENT APPROACH FOR FREE SURFACE FLOWS USING UNSTRUCTURED GRIDS

Laura Battaglia, Mario A. Storti and Jorge D'Elía

Centro Internacional de Métodos Computacionales en Ingeniería (CIMEC), Instituto de Desarrollo Tecnológico para la Industria Química (INTEC), Universidad Nacional del Litoral - CONICET , Güemes 3450, 3000-Santa Fe, Argentina, e-mail: lbattaglia@santafe-conicet.gov.ar, web page: http://www.cimec.org.ar

Keywords: fluid mechanics, free surface flows, interface capturing, level set, finite elements, unstructured grids.

Abstract. An interface-capturing finite element method based on the level set approach is proposed for solving free surface incompressible fluid flows, especially those that are hard to model through an interface-tracking technique, like the one presented in previous works (Battaglia *et al.*, "Stabilized Free Surface Flows", in Mecánica Computacional, Vol. XXVI, 2007). The methodology is developed in the PETSc-FEM code (http://www.cimec.org.ar/petscfem) in order to solve the Navier-Stokes equations for the fluid state and the advection of the level set function which gives the free surface position. Some examples solved by this method are presented, including the collapse of a liquid column problem.

1 INTRODUCTION

Free Surface (FS) flows are a particular type of flow with moving interfaces, which can be either stationary or transient. Typical examples with FS are open channels, sloshing in transport tanks or the wave pattern generated by a ship. Problems like those motivate the numerical simulation of such flows, in this particular case through the Finite Element Method (FEM).

The complexity of mobile interfaces is due to different reasons, but the main issue is that the FS position, which is *a priori* unknown, is also part of the solution (Shyy et al., 1996). Then, a classic Eulerian representation for solving a flow problem is insufficient because the flow domain suffers shape changes during time evolution.

By the other side, in Lagrangian methods the FS is specifically defined, *i.e.* over nodes or element sides in FEM, which allows a more precise tracking for the FS and its physics, originating the so called *interface-tracking* methods. These alternatives are also very limited, mostly because large relative deformations are accumulated along the evolution of the problem, which is very hard to handle with FEM, including or not remeshing procedures during the simulation.

As the classic representations themselves were not prepared to handle certain interfacial problems, some procedures were developed by combining Eulerian and Lagrangian methods. As an example, the *Arbitrary Lagrangian-Eulerian* (ALE) (Huerta and Liu, 1988; Donea and Huerta, 2003) is one of the most populars. In the ALE scheme, the FS boundary deformation is followed in a Lagrangian way, while the interior nodes are moved with some criteria that avoids an excessive distortion of the mesh elements. This rezoning implies that the mesh velocity must be taken into account while solving the fluid state equations, but higher precision in comparison to other approaches is reached at the interface. As a disadvantage, phenomenas like wave breaking, very large FS deformations or similar ones lead to a failure of the method. This technique is frequently used in sloshing problems (Souli and Zolesio, 2001), and was studied before in Battaglia et al. (2007) and Battaglia et al. (2006).

From an Eulerian point of view, interface problems are faced through *interface-capturing* methods, such as *Volume of Fluid* (VOF) (Hirt and Nichols, 1981; Scardovelli and Zaleski, 1999) and *Level Set method* (LS) (Sethian, 1995), where the mesh is fixed but the domain includes both liquid and gas phases in FS problems, in such a way that the interface cuts a strip of elements. Main associated drawbacks are related to mass conservation of the phases involved, boundary conditions over the interface and the FS reconstruction, which is "captured" according to the data in its neighborhood. VOF and LS schemes are nowadays very popular, separately (Löhner et al., 2006) or combined (Sussman and Puckett, 2000).

In this work, a LS-like procedure for solving FS flows implemented through the PETSc-FEM (2008) code is presented, which is based on the Message Passing Interface (MPI, 2008) and Portable Extensible Toolkit for Scientific Computation (PETSc) (Balay et al., 2005) libraries for parallel computing.

The kind of problems solved in this work are included in different areas, such as Hydraulic or Mechanical Engineering, but considering that physical dimensions are large enough in order to neglect interfacial tension effects. Besides, the fluids are considered viscous, incompressible, with Newtonian behavior and constant physical properties.

2 GOVERNING EQUATIONS

The following sections describe step by step the interface capturing method proposed. First, a "classic" LS formulation is summarized as a background for the following sections, as Sec.

2.2, which describes the fluid flow equations to be solved. Finally, Sec. 2.3 explains the present approach for following the FS evolution, considering some new ideas in order to improve the level set function update.

2.1 Level set formulation

The LS formulation consists of the definition of a level set function ϕ over the whole domain Ω, i.e. both the liquid and the gas phases, in time $t \in [0, T]$. This function is given as in Sussman and Smereka (1997),

$$\phi(\mathbf{x}, t) = \begin{cases} > 0 & \text{if} \quad \mathbf{x} \in \Omega_l; \\ = 0 & \text{if} \quad \mathbf{x} \in \Gamma; \\ < 0 & \text{if} \quad \mathbf{x} \in \Omega_g; \end{cases} \tag{1}$$

where $\mathbf{x}$ indicates the spatial position in which the function is evaluated, either over the subdomain Ω_l corresponding to the liquid phase, or over Ω_g for the gaseous region, being $\Omega = \Omega_l \cup \Omega_g$. Note that the subindex l is associated to the liquid phase and subindex g to the gaseous one, nomenclature that will be kept for the rest of this work. Finally, the interface is defined as the set

$$\Gamma_{\mathrm{I}} = \{\mathbf{x} | \phi(\mathbf{x}, t) = 0\}. \tag{2}$$

For free surface problem, $\Gamma_{FS} = \Gamma_{\mathrm{I}}$ is adopted.

One of the purposes of the method proposed in Sec. 2.3 is keeping ϕ bounded, in particular $|\phi| \leq 1$, as will be stated in Sec. 2.2.

2.2 Fluid flow problem

The fluid flow problem to be solved is represented by the incompressible form of the Navier-Stokes (NS) equations, i.e. considering that both fluids are incompressible,

$$\begin{aligned} \rho(\phi(\mathbf{x}, t)) \left(\partial_t \mathbf{v} + \mathbf{v} \cdot \nabla \mathbf{v} - \mathbf{f}\right) - \nabla \cdot \boldsymbol{\sigma} = 0 \, ; \\ \nabla \cdot \mathbf{v} = 0 \, ; \end{aligned} \tag{3}$$

for $\mathbf{x} \in \Omega$, where $\mathbf{v}$ is the fluid velocity, $\mathbf{f}$ is the body force, $\rho(\phi(\mathbf{x}, t))$ is the fluid density, which depends on both the position $\mathbf{x}$ and the evaluation time t because of the multiphase proposal, and $\partial_t(...) = \partial(...)/\partial t$ indicates the partial time derivative. The fluid stress tensor $\boldsymbol{\sigma}$ is decomposed into an isotropic $-p\mathbf{I}$ and a deviatoric part $\mathbf{T}$,

$$\boldsymbol{\sigma} = -p\mathbf{I} + \mathbf{T} \, ; \tag{4}$$

with p the pressure, $\mathbf{I}$ the identity tensor and $\mathbf{T}$ a linear function of the strain rate tensor $\boldsymbol{\epsilon}$. Considering only Newtonian fluids,

$$\begin{aligned} \mathbf{T} &= 2\, \mu(\phi(\mathbf{x}, t))\, \boldsymbol{\epsilon} \, ; \\ \boldsymbol{\epsilon} &= \frac{1}{2} \left[\nabla \mathbf{v} + (\nabla \mathbf{v})^T\right] \, ; \end{aligned} \tag{5}$$

where $(...)^T$ indicates transposition. The dynamic and kinematic fluid viscosities are respectively $\mu = \mu(\phi(\mathbf{x}, t))$ and $\nu(\phi(\mathbf{x}, t)) = \mu(\phi(\mathbf{x}, t))/\rho(\phi(\mathbf{x}, t))$, which depend on the level set function ϕ in order to take into account the phases involved.

The flow conditions over the domain boundaries Γ in the cases considered up to now are $\mathbf{v} = \mathbf{v}_{\text{wall}}$ over Γ_{wall}, being Γ_{wall} the solid boundaries, and periodic boundary conditions for other cases. The pressure is imposed as $p = 0$ over the top of the domain.

As in most LS schemes, density and viscosity values are determined as functions of the LS values in the following way,

$$\begin{aligned} \rho(\phi) &= \frac{1}{2}\left[\left(1+\tilde{H}(\phi)\right)\rho_l + \left(1-\tilde{H}(\phi)\right)\rho_g\right]; \\ \mu(\phi) &= \frac{1}{2}\left[\left(1+\tilde{H}(\phi)\right)\mu_l + \left(1-\tilde{H}(\phi)\right)\mu_g\right]. \end{aligned} \tag{6}$$

In particular, in the neighborhood of the interface Γ_{FS} there is a region defined by a distance ε, where ϕ varies in a continuous way from $+1$ to -1, giving a ϕ-field easier to solve for the advection stage. This strip is also needed in order to define a smooth transition between the liquid and the gas; otherwise, the discontinuity in the properties would cause numerical problems. In spite of that, the strip is allowed to be thinner than in the former case, as reported by Sussman and Smereka (1997) and others. In this proposal, $\tilde{H}(\phi)$ is calculated as

$$\tilde{H}(\phi) = \begin{cases} 1 & \text{if} \quad |\phi| > \tilde{\varepsilon}; \\ \tanh\left(\frac{\pi\phi}{\tilde{\varepsilon}}\right) & \text{if} \quad |\phi| \leq \tilde{\varepsilon}; \end{cases} \tag{7}$$

i.e., for $|\phi| \to \tilde{\varepsilon}$ is $\tilde{H}(\phi) \to 1$, with an adopted $\tilde{\varepsilon} = 0.5$ which lead to a strip of a half of ε the one for the ϕ variation. As an alternative to the smooth transition, some authors use the *Ghost Fluid Method* (Caiden et al., 2001), which implicitly introduces the jump conditions at the interface.

2.3 Advection of the level set function

The velocity field $\mathbf{v}$, continuous across the interface, generates the advection of Γ_{FS}, which is the same as the advection of $\phi(\mathbf{x}, t)$,

$$\partial_t \phi + \mathbf{v} \cdot \nabla\phi = 0; \tag{8}$$

where Dirichlet boundary conditions are given by

$$\phi = \bar{\phi} \qquad \text{over} \quad \Gamma_{\text{in}}; \tag{9}$$

being the inflow section $\Gamma_{\text{in}} = \{\Gamma |\ \mathbf{v} \cdot \mathbf{n} > 0\}$. Due to the hyperbolic character of the problem, no other boundary condition is needed, althoug periodic ones are considered in some of the examples.

Instead of the problem given in Eq. (8), a different formulation is introduced with the aim of improve the transport of the $\phi = 0$ curve by adding the Right Hand Side (RHS) terms of the following expression,

$$\partial_t \phi + \mathbf{v} \cdot \nabla\phi = C_r\ \phi\ (\phi_{\text{ref}}^2 - \phi^2) - \kappa(\phi)\Delta\phi; \tag{10}$$

where the RHS is null over the interface and enforces the condition $\phi = \pm\phi_{\text{ref}}$ outside the interpolating strip, being boundary conditions the same as in the former case. The resulting problem is an advective one plus a source and a diffusive terms. The user chosen constant C_r, or *regularizing parameter*, is given in units of time^{-1}, Δ is the Laplacian operator and $\kappa(\phi)$ is

a diffusion parameter calculated as $\kappa(\phi) = \kappa_{\text{ref}} \ \min(|\phi|/\phi_{\text{ref}}, 1)$, which acts over most of the field but decreases to 0 near $\phi = 0$, with κ_{ref} also adopted by the user.

Reference values are $\phi_{\text{ref}} = 1$ and $\kappa_{\text{ref}} = (\varepsilon/h)^2 \ h^2 \ C_r$, in $\text{length}^2/\text{time}$ units, where h characterizes the mesh element size and ε/h indicates how many elements are involved in one half of the interpolation region in order to keep it constant along the analysis.

This problem is solved through a new linear finite element called "smoke" and programmed as part of the PETSc-FEM code. This element consist of a typical advection element plus the reactive and diffusive terms, allowing the resolution of Eq. (10) by the PETSc-FEM advection-diffusion FEM solver, stabilized with streamline upwind/Pétrov-Galerkin (SUPG) (Brooks and Hughes, 1982). In case $C_r = 0$, the program only solves Eq. (8), but also stabilized with SUPG. An important issue is that the method was programmed in such a way that two and three-dimensional problems can be easily solved.

A test case for estimating the performance of this methodology is shown in Sec. 4.1, where the "smoke" approach is compared to the results obtained with $C_r = 0$.

2.4 Reinitialization

The methodology presented up to now does not count on a reinitialization step, which is usually made for conserving the ϕ profile across the interface by solving a redistancing problem to the $\phi = 0$ curve. The thesis presented by Hysing (2007) made an interesting summary about this subject, and some spread procedures are those presented by Sussman and Smereka (1997), Parolini (2004), or Adalsteinsson and Sethian (1999). At this point, note that most LS methods work with ϕ values not restricted to the interval $[-1, 1]$, as in this case.

In the works of Olsson and Kreiss (2005) and Olsson et al. (2007), redistancing is made through the resolution of a problem to steady state after each pure advection step, given by

$$\partial_\tau \phi + \nabla \cdot [\phi(1-\phi)\mathbf{n}] = \hat{\mu} \nabla \cdot [(\nabla\phi \cdot \mathbf{n})\mathbf{n}] \,; \tag{11}$$

which is similar to the one proposed in Eq. (10), with $\hat{\mu} = \mathcal{O}(h)$ and τ an artificial time. Regarding this, the possibility of split Eq. (10) in two partial differential equations, one for the transport of ϕ and the other one as a regularizing operator, is being evaluated. Nowadays, the reinitialization procedure is being developed because it is needed due to the mass loss and the smoothing of the interface registered in the solved examples, but results are not yet available.

3 ALGORITHM

The algorithm proposed for the numerical solution of each of the problems from Secs. 2.2 and 2.3 is a weak coupling between the two FEM solvers, whose iterative procedure is sketched in Figure 1. Both the NS and the ADVDIF processes require initial conditions for the beginning of the procedure, but from the first iteration the task of each solver is as follows,

- **NS**: solves the fluid flow problem of Eq. (3) for some time t^n, after n time steps, considering $\rho = \rho(\phi(\mathbf{x}, t))$ and $\mu = \mu(\phi(\mathbf{x}, t))$, i.e. the ϕ field is known, and, once the step is finished, transmits the calculated fluid velocities over the whole domain Ω to the following stage, by nodes;

- **ADVDIF**: solves the advection-diffusion-reaction, Eqs. (8) or (10) depending on the value given to C_r, in time t^n by taking the fluid velocities from NS and sending back the new level set function values, also by nodes, which allow the calculation of the fluid state in t^{n+1}.

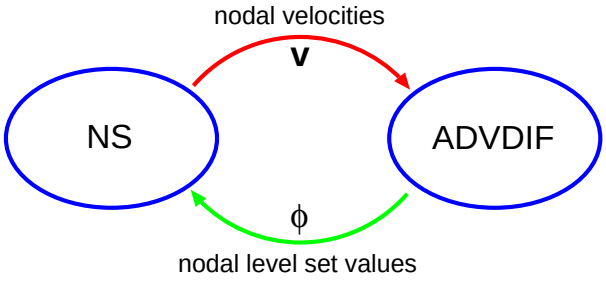

Figure 1: Weak coupling between processes for solving the level set / fluid flow problem.

In case a reinitialization step proves to be necessary, the iterative algorithm would include a third instance which would process the level set ϕ nodal values after the ADVDIF stage, but probably not every time step.

4 NUMERICAL EXAMPLES

As mentioned before, the method is able to solve two and three-dimensional problems, but due to the high costs of the last ones the examples to be presented are two-dimensional. Either way, the conclusions extracted are valid for the evaluation of certain aspects to be improved.

4.1 Advection of ϕ

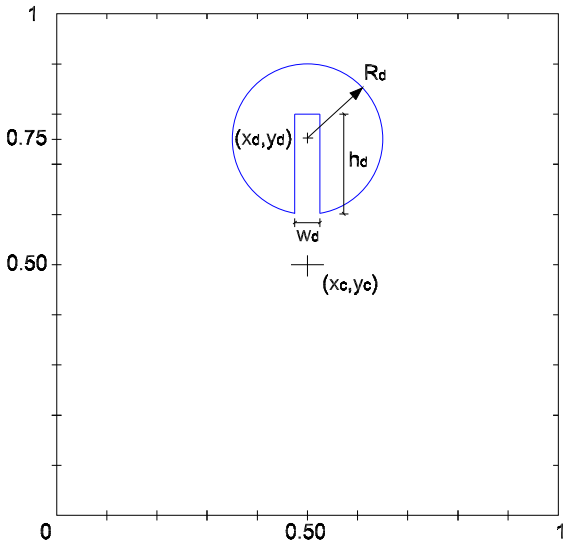

Figure 2: Domain and shape of $\phi = 0$ for the the Zalesak's disk test.

The effectiveness of the advection procedure is tested over the *Zalesak's* disk (Zalesak, 1979), which is a reference for many publications about this subject, see Mut et al. (2006), Sussman and Puckett (2000) or Di Pietro et al. (2006). The test consist of a circle with a slot inside a square domain, see Fig. 2, where the radius is $R_d = 0.15$ m, it is centered at $(x_d, y_d) = (0.5, 0.75)$ m and the notch is $w_d = 0.05$ m width and $h_d = 0.25$ m height. This disk

rotates with the velocity field given by its cartesian components

$$\begin{aligned} v_x &= 2\pi\,(y - y_c)\,; \\ v_y &= -2\pi\,(x - x_c)\,; \end{aligned} \tag{12}$$

i.e., it is a rigid rotation around the point $(x_c, y_c) = (0.5, 0.5)$ m. After one revolution, for a final time of $t_f = 1$ s and time step of $\Delta t = 1/(200\pi)$ s ≈ 0.0016 s, the quality of the numerical solution is compared to the theoretical one, which is the same as the initial condition.

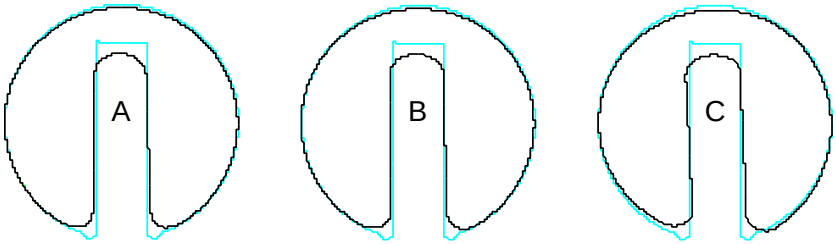

Figure 3: Initial (cyan) and final stages (black) in cases A, B and C for the Zalesak's disk.

The problem was solved over a structured mesh composed by 80000 linear triangles, considering three main cases,

Case	C_r [s^{-1}]
A	0
B	1
C	10

The artificial diffusion parameter κ_{ref} is taken as in Sec. 2.3. The changes on the zero level set ($\phi = 0$) for all the cases are plotted in Fig. 3, where it is possible to identify the common weaknesses, which are the smoothing of marked corners. Case A is the most "diffusive", as observed at the top of the notch, while C seem to be late, i.e., as if rotating velocity was lower.

Regarding area conservation of the $\phi > 0$ region, there are few differences among the alternatives given, being $\Delta A_{\text{A}} = 1.9\%$, $\Delta A_{\text{B}} = 1.9\%$ and $\Delta A_{\text{C}} = 2.8\%$.

Besides the plane shape of the $\phi = 0$ curve and mass conservation, another aspects will be evaluated in order to decide whether the "smoke" element is convenient for the LS function advection. In Fig. 4, there are representations of the ϕ profiles obtained for a section at $y = 0.70$ m in cases A, B and C. The curves observed in Fig. 4 show that, even when $\phi = 0$ is well tracked, the amplitude of the LS function was reduced not only at positive maximum but also in $x \approx 0.5$ m. This situation is also registered in case B, although the peaks are not as reduced as in the former case. Finally, for $C_r = 10$ s^{-1}, the initial curve is very well tracked in the section, but small undershoots and overshoots are registered. The importance of this analysis is related to the fact that the "smoke" element should be employed to advect ϕ, which is used by the NS solver to define the liquid or gas properties, as stated in Eq. (6). Then, inaccuracies in the values of the LS function will lead to inaccurate results in the fluid problem and the failure of the method, regarding precision.

As none of the three alternatives shows a completely satisfactory behavior, it is clear the importance of a reinitialization instance over the LS field, which is not implemented yet. Even though, the resolution of this kind of problems with $C_r > 0$ could be a useful tool for reducing the reinitialization costs.

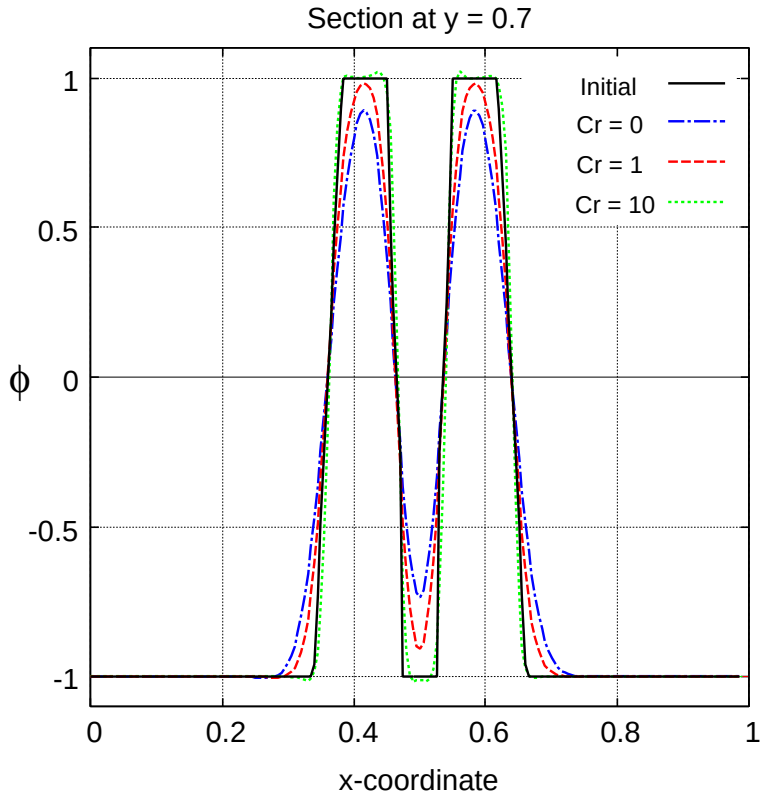

Figure 4: Initial and final profiles for the Zalesak's disk: section at $y = 0.70$ m.

4.2 Validation problem for FS: small displacements

The interface-capturing method proposed in this work is developed for large free surface displacements, but for small displacements it is also necessary a validation. For this task, the selected problem consist of the motion of the interface between two viscous fluids with a wave as an initial condition, whose amplitude is damped by the fluid viscosity during time evolution. The analytical expression for the displacement of the interface position over the left limit was given by Prosperetti (1981).

The domain of analysis proposed is rectangular, with width L and height $H = H_l + H_u$, being H_l the inferior liquid height and H_u upper one, as seen in Fig. 5, with the initial wave amplitude a_0 negligible compared to H. The lateral boundaries are related by periodic boundary conditions for simulating the infinite lateral domain for both of the solving instances. Finally, perfect slip conditions for the fluid flow are adopted in both bottom and top of the region and pressure $p = 0$ over the last one, while for the advection problem these are $\phi = 1$ and $\phi = -1$, respectively, see again Fig. 5. The1 initial condition for the free surface $\phi = 0$ is given by

$$h(x) = H_l + a_0 \cos(2\pi x/L) \; . \tag{13}$$

The system is submitted to a gravity acceleration g, and each fluid count on its own properties, density ρ_l and kinematic viscosity ν_l for the lower liquid, and the corresponding ρ_u and ν_u for the other one.

The analytical expression describing the vertical displacement of the interface as a function of time t for small amplitude flat waves in an infinite depth domain is known if the kinematic

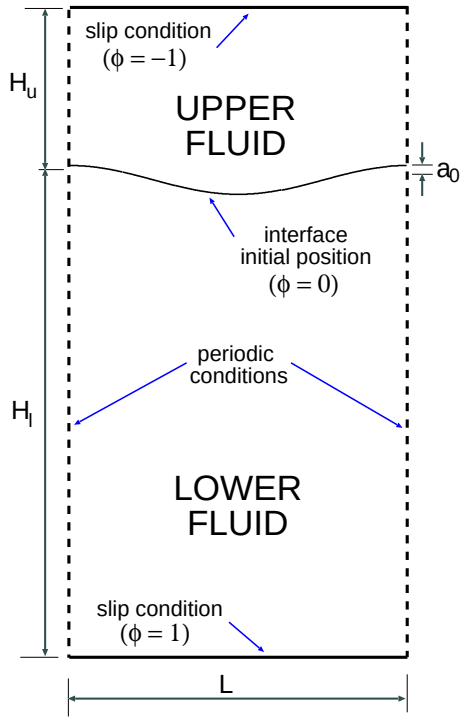

Figure 5: Geometrical data and boundary conditions for the small displacements test.

viscosities of both fluids are the same, i.e., $\nu = \nu_l = \nu_g$, and is as follows,

$$a(t) = \frac{4(1-4\beta)\nu^2 k^4}{8(1-4\beta)\nu^2 k^4 + {\omega_0}^2}\, a_0\, \text{erfc}(\nu k^2 t)^{1/2} + \\ + \sum_{i=1}^{4} \frac{z_i}{Z_i} \left(\frac{\omega_0^2 a_0}{z_i^2 - \nu k^2} \right) \exp[(z_i^2 - \nu k^2)t]\, \text{erfc}(z_i t^{1/2}) \; ; \tag{14}$$

where the density parameter β is calculated as $\beta = \rho_l \rho_u / (\rho_l + \rho_u)^2$, k is the wave number, $\omega_0^2 = gk$ is the inviscid natural angular frequency, and each z_i is a root of the following algebraic equation,

$$z^4 - 4\beta(k^2\nu)^{1/2} z^3 + 2(1-6\beta)k^2\nu z^2 + 4(1-3\beta)(k^2\nu)^{3/2} z + (1-4\beta)\nu^2 k^4 + \omega_0^2 = 0;$$

with $Z_1 = (z_2 - z_1)(z_3 - z_1)(z_4 - z_1)$ and Z_2, Z_3, Z_4 calculated by circular permutation of the indices. The expression erfc$(...)$ is the error function for complex variable.

The numerical resolution was performed over a domain defined by $H_l = 1.50$ m, $H_u = 0.50$ m and $L = 1.00$ m, and an initial amplitude $a_0 = 0.03$ m, which is introduced as an initial ϕ field for the problem (10) with $\varepsilon \approx 0.08$ cm, considering that $h \approx 0.005$ cm is a representative mesh size for the region closer to the interface. The domain was discretized with an unstructured finite element mesh which consist of about 11240 linear triangular elements generated by a meshing program developed by Calvo (2005). The gravity acceleration considered is $g = 1$ m/s^2, densities are $\rho_l = 100$ kg/m^3 and $\rho_u = 1$ kg/m^3, kinematic viscosity is $\nu = 0.0001$ m^2/s and the final time $t_f = 10.0$ s, with $\Delta t = 0.0125$ s. This problem was solved for two values of the regularizing parameter $C_r = 0$ and $C_r = 0.5$ s^{-1}, using an implicit scheme for time integration.

The results obtained are plotted in Fig. 6, where the numerical cases are $C_r = 0.5$ s^{-1} for the "smoke" approach and $C_r = 0$ for the ordinary advective problem, plotted together with

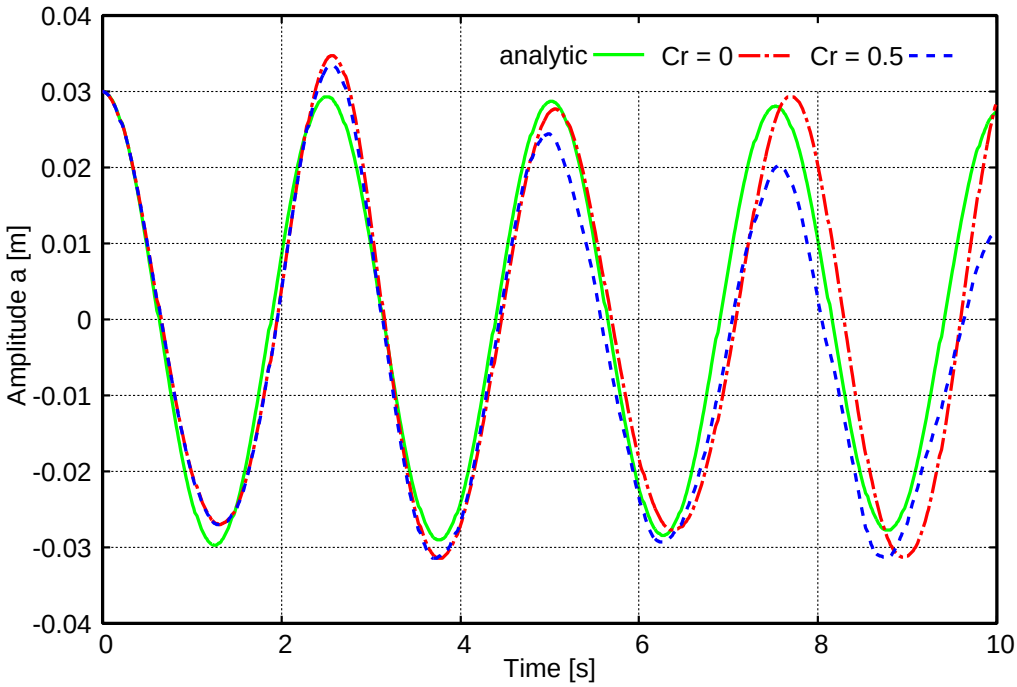

Figure 6: Vertical displacement of the interface over the left side for small displacements.

the analytical curve. These curves show that phase is respected by the $C_r = 0.5\ \mathrm{s}^{-1}$ curve but amplitude is not well tracked by neither of the numerical solutions for $t > 5$ s. Mass conservation was controlled for both cases, but the losses were negligible because of the small amplitude of the displacements.

As well as in the former example, two final profiles of the level set function obtained after 100 time steps for different values of C_r are compared, see Fig. 7. When $C_r = 0$, corresponding to the stabilized advective solution, the transition strip shows different widths for the liquid and the gaseous phases, being in this case $\varepsilon_0^l < \varepsilon_0^g$, following the notation given in this figure. By the other side, when adopting $C_r = 1\ \mathrm{s}^{-1}$ the resolution is made with the "smoke" element, proving that the ϕ profile keeps the initial width at the transition, with $\varepsilon_1^l \approx \varepsilon_1^g$, and a smooth variation between $\phi = +1$ and $\phi = -1$, which allows a better interpolation for the fluid properties at the NS resolution instance. This comparison lead to conclude that $C_r > 0$ and $\kappa = \kappa(\phi)$ are helpful for regularizing the profile of ϕ regarding the conservation of ε and the smoothness of the transition, respectively.

4.3 Collapse of a liquid column

The last example to be presented consist of the collapse of a water column inside an air atmosphere similar to those presented in numerous works related to FS simulations, like Cruchaga et al. (2007) or Maronnier et al. (1999), with an aspect ratio of $r_a = 2$, see sketch in Fig. 8. The domain Ω is $W_d = 4$ m wide and $H_d = 3$ m height, while the water column is defined by $W_c = 1$ m and $H_c = 2$ m.

The fluid properties are the corresponding ones for water in the liquid phase, being density $\rho_l = 1000\ \mathrm{kg/m^3}$ and dynamic viscosity $\mu_l = 1.0 \times 10^{-3}\ \mathrm{kg/(m\,s)}$, and for the gaseous one, they are $\rho_g = 1\ \mathrm{kg/m^3}$ and $\mu_g = 1.0 \times 10^{-5}\ \mathrm{kg/(m\,s)}$, respectively.

Boundary conditions for the NS problem are slip all over the contour, i.e. $\mathbf{v} \cdot \mathbf{n} = 0$ with $\mathbf{n}$ the vector normal to the wall, see Fig. 8, and pressure imposed $p = 0$ at the top. The ADVDIF

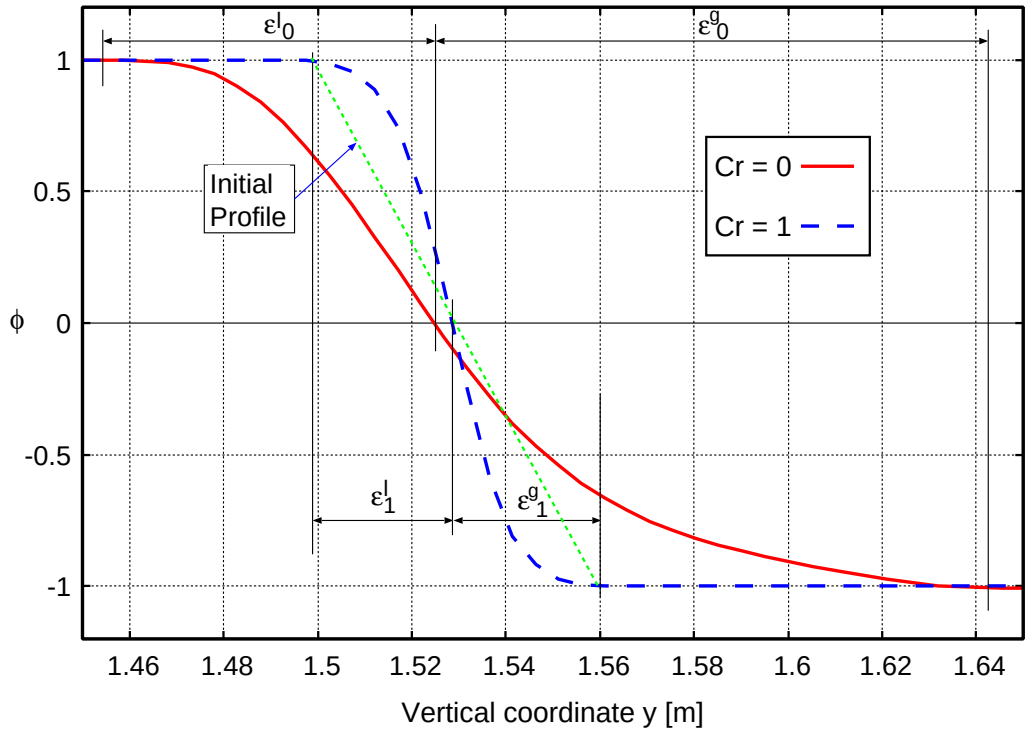

Figure 7: Small displacements. Variation of ϕ across the interface for different values of C_r and reference profile in a section over the left side of the domain.

problem has no imposition over ϕ because there is not inflow section. Considering the initial conditions, as both fluids are at rest is $\mathbf{v}_0 = \mathbf{0}$ in the fluid problem, and the map of ϕ is defined in such a way that nodes corresponding to the column of water verify $0 < \phi \leq 1$ and the rest of them are included inside the interval $-1 \leq \phi < 0$, being $\phi = 0$ at the FS initial position. Once the analysis is started, the column of water is affected by the imposed gravity acceleration of $g = 9.81\ \mathrm{m/s^2}$ and it starts to collapse.

The computational simulation was performed up to a final time $t_f = 10\ \mathrm{s}$ during 2000 time steps with a time stepping of $\Delta t = 0.005\ \mathrm{s}$ and implicit integration for both instances of the algorithm. The spatial finite element mesh is composed by quad elements with sides of $h = 0.033\ \mathrm{m}$, conforming a structured grid of about 11000 nodes, which are the same for the

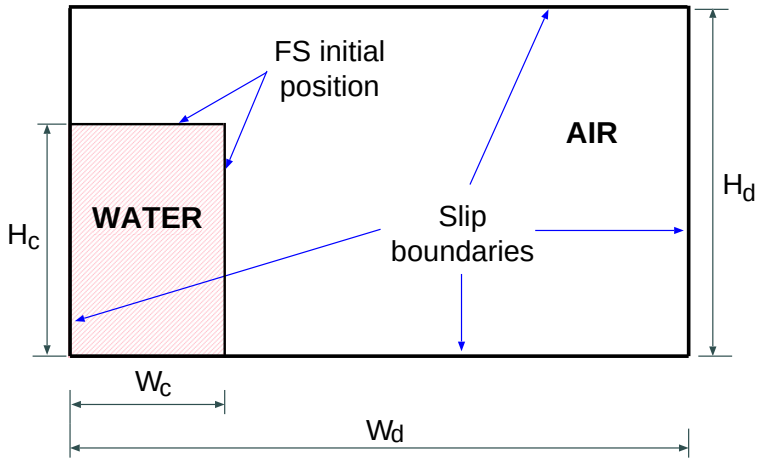

Figure 8: Geometry for the problem of the water column collapse.

NS and the ADVDIF solvers. The parameters adopted for the "smoke" element are $C_r = 1\ \mathrm{s}^{-1}$ and $\kappa_{ref} = 0.01\ \mathrm{m}^2/\mathrm{s}$, the last one calculated from the transition width of $\varepsilon = 0.10\ \mathrm{m}$.

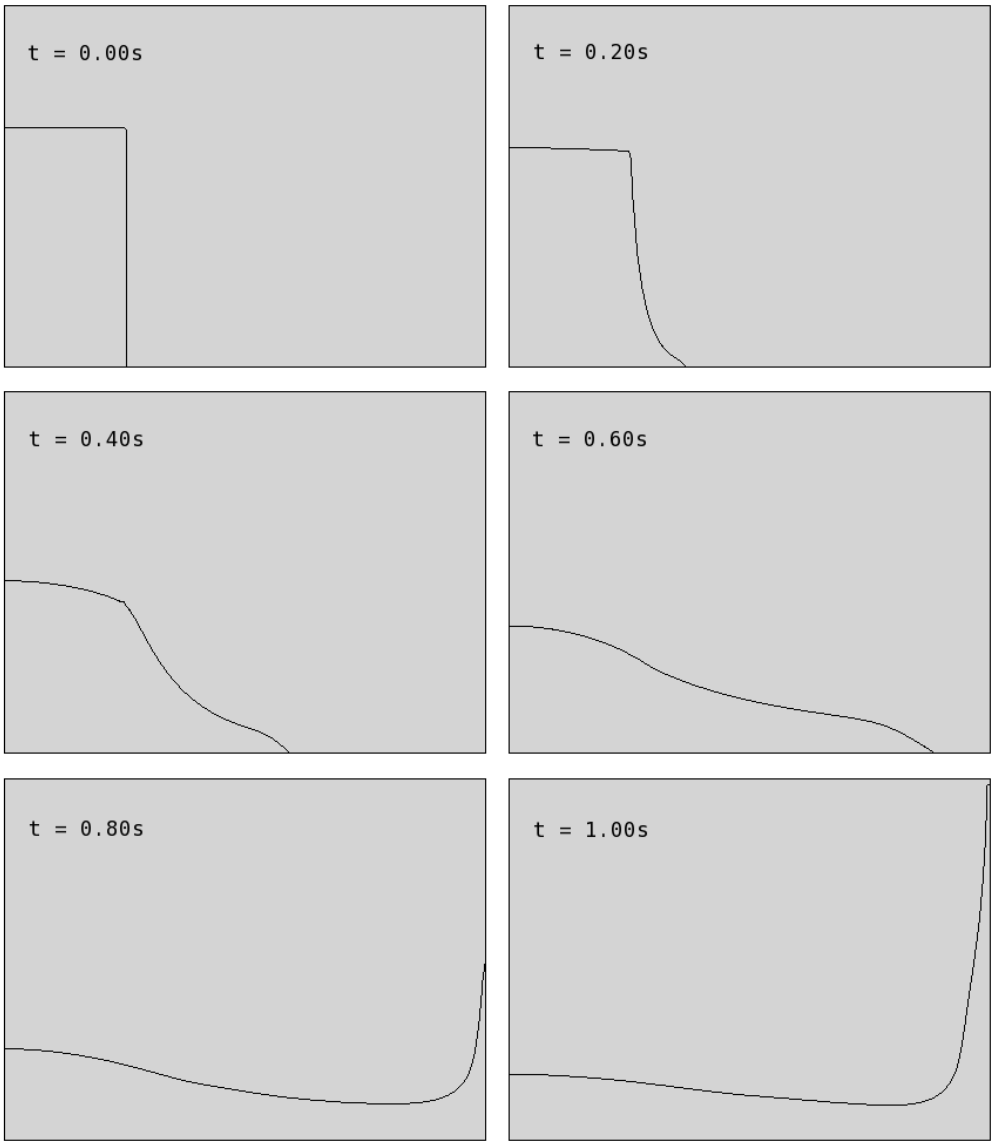

Figure 9: Early stages for the collapse of the liquid column.

Results are plotted in Figs. 9 to 11, where the interface is represented by the black line. As it is possible to see, there are three stages at this problem, the first of them is the collapse of the column, or "early stage" in Fig. 9, the second one is developed after the water impacts the right side of the domain up to $t \approx 2.75\ \mathrm{s}$, see Fig. 10, and the last one is registered from that time up to the simulation end, identified as "final stage" in Fig. 11. The collapse stage shows good agreement with similar numerical or experimental results, see Cruchaga et al. (2007), but the other ones are very hard to check due to the few available results, the splash of the liquid and the bubbles generated and dissolved, especially when some unphysical phenomena, like air originated at the bottom or disappearing droplets, are registered, as seen in the last figure.

The level set function field is plotted in Fig. 12 for three time steps, each of them corresponding to one of the stages mentioned before. The main difference among them is related to

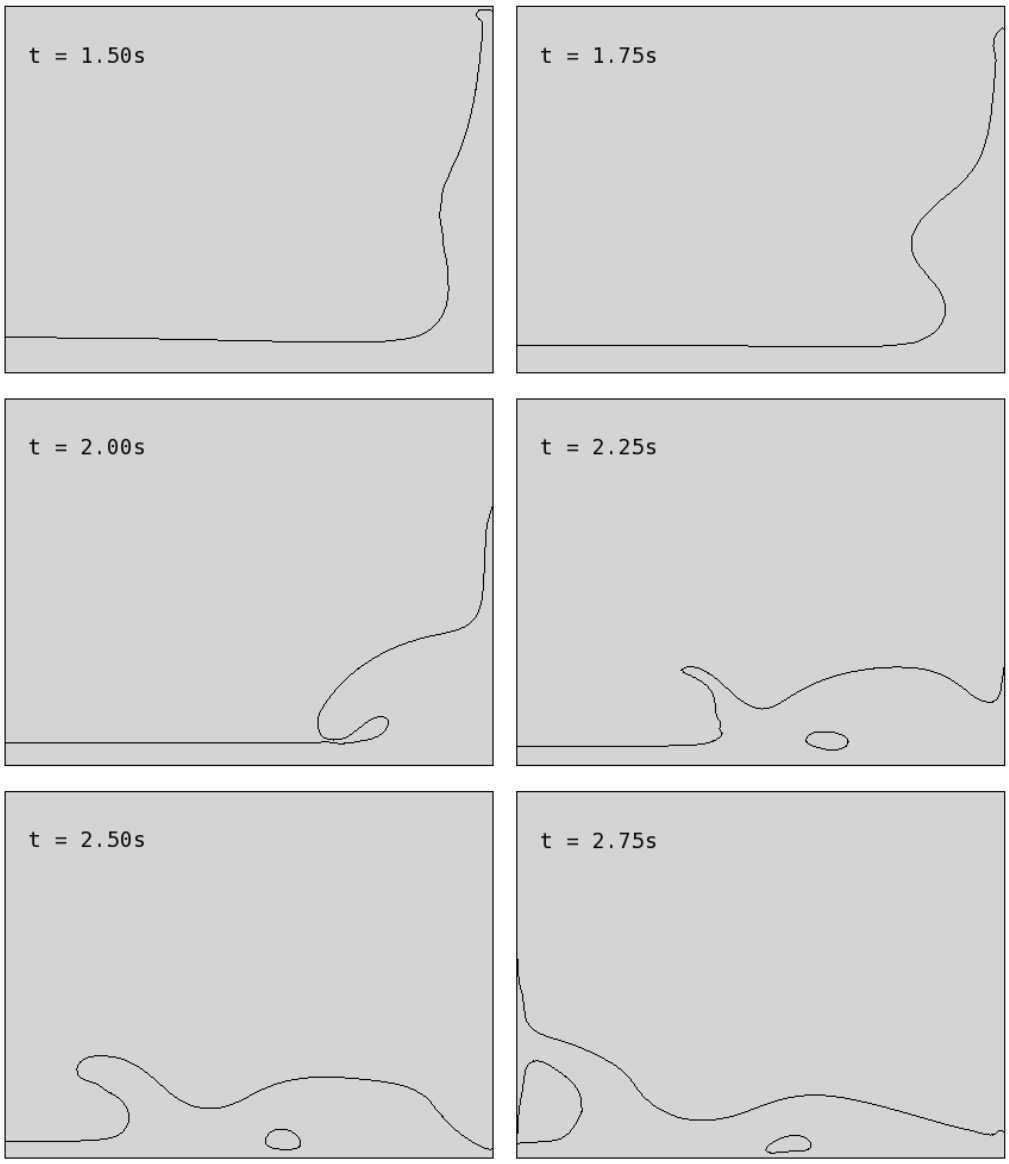

Figure 10: Intermediate steps for the collapse of the liquid column.

the "thickness" of the interface, which is lower in the picture for $t = 0.60$ s. For middle stages, the parameter ε is no longer representative of the interface transition, which is more evident at the central peak and its vortex. Finally, for $t = 4.75$ s, the ϕ field is much more spread due to the accumulated error along the simulation and the absence of a reinitialization procedure that could improve the results.

5 CONCLUSIONS

It is clear that the methodology implemented is not totally satisfactory in its current state. This affirmation is based on the analysis of the results showed, e.g. the slight loss of shape in Sec. 4.1, the inaccuracies in following the free surface displacements after certain number of time steps from Sec. 4.2, or some unphysical behavior appeared in breaking FS problems, appreciated in Sec. 4.3. In spite of that, the NS and the ADVDIF instances show numerical robustness, even for tight transition strips in ϕ and, as a consequence, for pronounced fluid properties variations. Besides, the smoothing properties given by the "smoke" element after

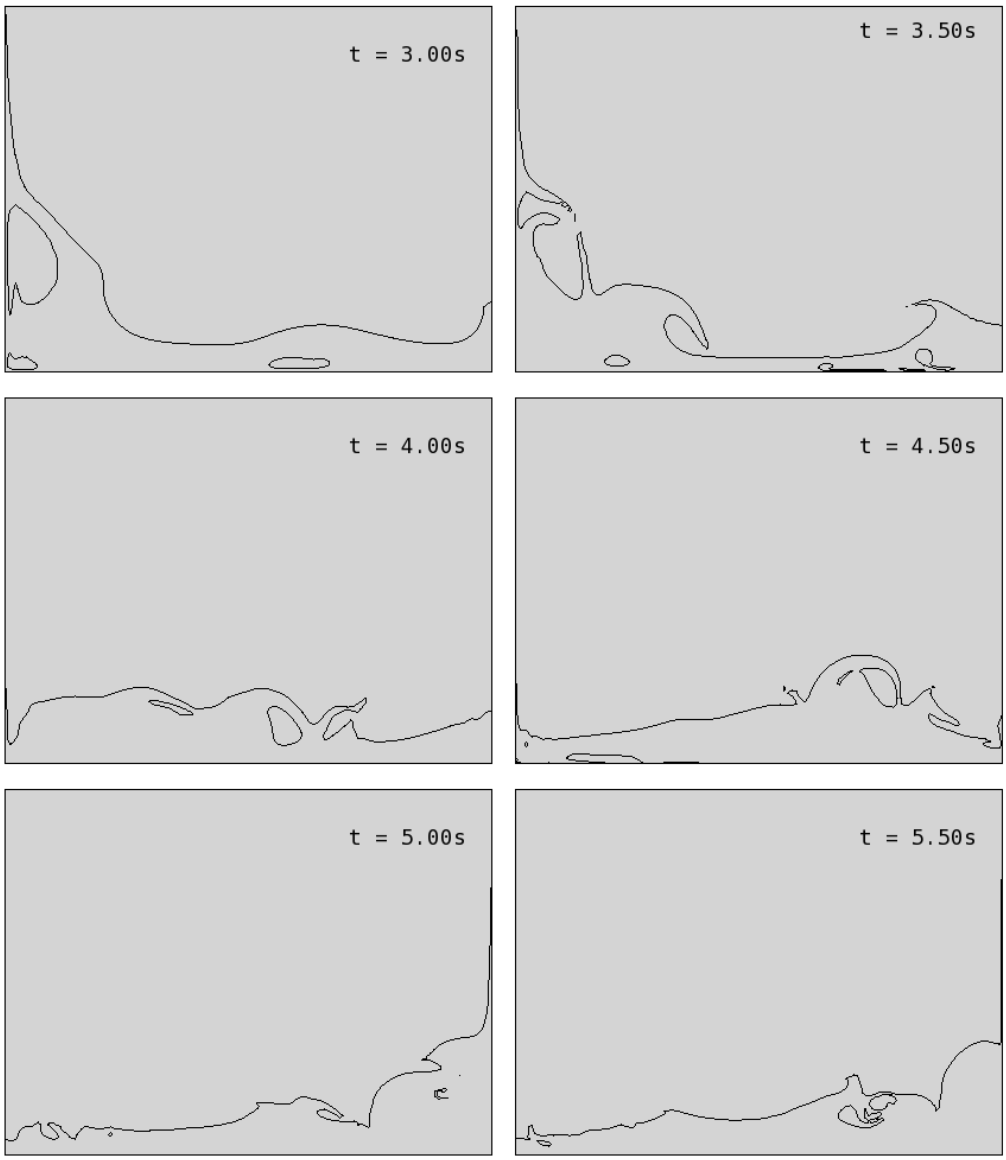

Figure 11: Final stages in the problem of collapse of the liquid column. Bubbles and droplets evolution.

each time step is good, considering the conservation of the level set profile across the interface which enforces FS capturing, although this is hard to respect for long time simulations. Regarding these facts, a reinitialization procedure is being developed as well as the NS and the ADVDIF processes, and the interaction between them, are under revision. Other important issue is that turbulence is not modeled in this analysis, and neither are surface tension effects, introducing additional uncertainties to the model that would be considered as future work.

Acknowledgments This work has received financial support from Consejo Nacional de Investigaciones Científicas y Técnicas (CONICET, Argentina, grants PIP 02552/00, PIP 5271/05), Universidad Nacional del Litoral (UNL, Argentina, grant CAI+D 2005-10-64) and Agencia Nacional de Promoción Científica y Tecnológica (ANPCyT, Argentina, grants PICT 12-14573/2003, PME 209/2003, PICT 1506/2006), and was partially performed with the *Free Software Foundation GNU-Project* resources as GNU/Linux OS and GNU/Octave, as well as other Open Source resources as PETSc, MPICH, OpenDX, LaTeX and JabRef.

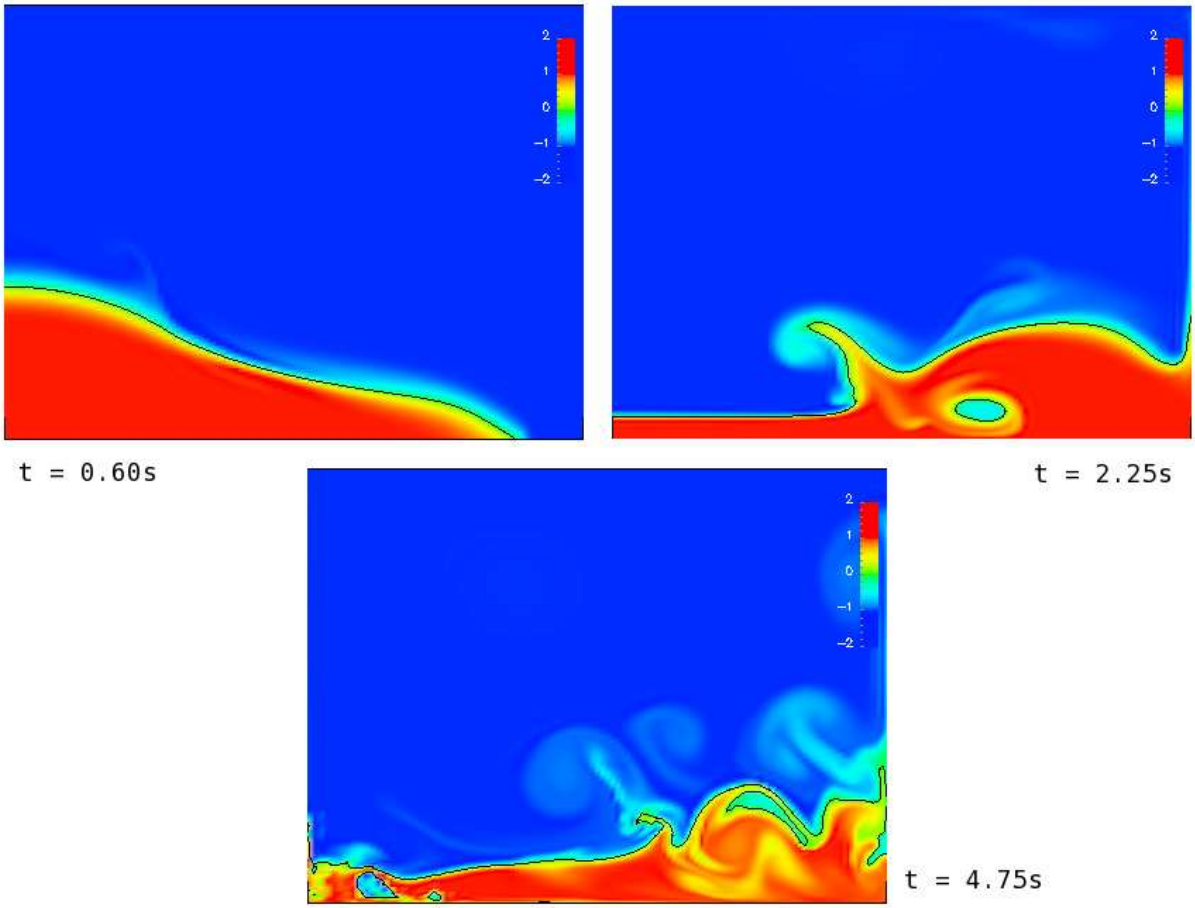

Figure 12: The level set field ϕ in the problem of the water column collapse for different stages.

REFERENCES

Adalsteinsson D. and Sethian J.A. The fast construction of extension velocities in level set methods. *Journal of Computational Physics*, 148(1):2–22, 1999.

Balay S., Buschelman K., Eijkhout V., Gropp W., Kaushik D., Knepley M., McInnes L., Smith B., and Zhang H. PETSc 2.3.0 Users Manual. Technical Report UC-405, Argonne Nat. Lab., 2005.

Battaglia L., D'Elía J., Storti M., and Nigro N. Numerical simulation of transient free surface flows using a moving mesh technique. *Journal of Applied Mechanics*, 73(6):1017–1025, 2006.

Battaglia L., Storti M.A., and D'Elía J. Stabilized free surface flows. In *Mecánica Computacional*, volume XXVI. 2007.

Brooks A. and Hughes T.J.R. Streamline upwind/Petrov-Galerkin formulations for convection dominated flows with particular emphasis on the incompressible Navier-Stokes equations. *Computer Methods in Applied Mechanics Engineering*, 32:199–259, 1982.

Caiden R., Fedkiw R.P., and Anderson C. A numerical method for two-phase flow consisting of separate compressible and incompressible regions. *Journal of Computational Physics*, 166(1):1–27, 2001.

Calvo N.A. *Generación de mallas tridimensionales por métodos duales*. Ph.D. thesis, Facultad de Ingeniería y Ciencias Hídricas, Universidad Nacional del Litoral, 2005.

Cruchaga M.A., Celentano D.J., and Tezduyar T.E. Collapse of a liquid column: numerical

simulation and experimental validation. *Computational Mechanics*, 39:453–476, 2007.

Di Pietro D., Lo Forte S., and Parolini N. Mass preserving finite element implementations of the level set method. *Applied Numerical Mathematics*, 56:1179–1195, 2006.

Donea J. and Huerta A. *Finite Element Methods for Flow Problems*. John Wiley & Sons, 2003.

Hirt C.W. and Nichols B.D. Volume of fluid (VOF) method for the dynamics of free boundaries. *Journal of Computational Physics*, 39:201–225, 1981.

Huerta A. and Liu W.K. Viscous flow with large free surface motion. *Computer Methods in Applied Mechanics and Engineering*, 69:277–324, 1988.

Hysing S.R. *Numerical Simulation of Immiscible Fluids with FEM Level Set Techniques*. Ph.D. thesis, Dortmund - Germany, 2007.

Löhner R., Yang C., and Oñate E. On the simulation of flows with violent free surface motion. *Comput. Methods Appl. Mech. Engrg.*, 195(41-43):5597–5620, 2006.

Maronnier V., Picasso M., and Rappaz J. Numerical simulation of free surface flows. *Journal of Computational Physics*, 155(2):439–455, 1999.

MPI. Message Passing Interface. 2008. http://www.mpi-forum.org/docs/docs.html.

Mut F., Buscaglia G.C., and Dari E.A. New mass-conserving algorithm for level set redistancing on unstructured meshes. *Journal of Applied Mechanics*, 73(6):1011–1016, 2006.

Olsson E. and Kreiss G. A conservative level set method for two phase flow. *Journal of Computational Physics*, 210(1):225–246, 2005.

Olsson E., Kreiss G., and Zahedi S. A conservative level set method for two phase flow II. *Journal of Computational Physics*, 225(1):785–807, 2007.

Parolini N. *Computational Fluid Dynamics for Naval Engineering Problems*. Ph.D. thesis, École Polytechnique Fédérale de Lausanne, 2004.

PETSc-FEM. A general purpose, parallel, multi-physics FEM program. 2008. GNU General Public License (GPL), http://www.cimec.org.ar/petscfem.

Prosperetti A. Motion of two superposed viscous fluids. *Physic of Fluids*, 24(7):1217–1223, 1981.

Scardovelli R. and Zaleski S. Direct numerical simulation of free-surface and interfacial flow. *Annual Reviews in Fluid Mechanics*, 31:567–603, 1999.

Sethian J.A. A fast marching level set method for monotonically advancing fronts. National Academy of Sciences, 1995.

Shyy W., Udaykumar H.S., Rao M.M., and Smith R.W. *Computational Fluid Dynamics with Moving Boundaries*. Taylor and Francis, 1996.

Souli M. and Zolesio J.P. Arbitrary lagrangian-eulerian and free surface methods in fluid mechanics. *Computer Methods in Applied Mechanics and Engineering*, 191(3-5):451–466, 2001.

Sussman M. and Puckett E.G. A coupled level set and volume-of-fluid method for computing 3d and axisymmetric incompressible two-phase flows. *Journal of Computational Physics*, 162(2):301–337, 2000.

Sussman M. and Smereka P. Axisymmetric free boundary problems. *Journal of Fluid Mechanics*, 341:269–294, 1997.

Zalesak S.T. Fully multidimensional flux-corrected transport algorithms for fluids. *Journal of Computational Physics*, 31(3):335–362, 1979.